

1 **Title:** *Impairments of saccadic and reaching adaptation in Essential Tremor are linked to movement*  
2 *execution*

3 **Abbreviated title:** *Motor adaptation impairments in Essential Tremor*

4 Florence Blondiaux – 1 & 2

5 +32 10 47 80 36 – [florence.blondiaux@uclouvain.be](mailto:florence.blondiaux@uclouvain.be)

6 Louisien Lebrun – 2 & 3

7 +32 2 764 54 19 – [Louisien.lebrun@uclouvain.be](mailto:Louisien.lebrun@uclouvain.be)

8 Bernard J. Hanseeuw – 2, 3, 4 & 5

9 +32 2 764 54 19 – [bernard.hanseeuw@uclouvain.be](mailto:bernard.hanseeuw@uclouvain.be)

10 Frédéric Crevecoeur – 1 & 2

11 +32 10 47 80 36 – [Frederic.crevecoeur@uclouvain.be](mailto:Frederic.crevecoeur@uclouvain.be)

12 1- Institute for Information and Communication Technologies, Electronics and Applied  
13 Mathematics, UCLouvain, Avenue Georges Lemaitre 4-6, 1348 Louvain-la-Neuve, Belgium

14 2- Institute of Neuroscience, UCLouvain, Avenue E. Mounier 53, 1200 Brussels, Belgium

15 3- Neurology Department, Saint-Luc University Hospital, Avenue Hippocrate 10, 1200  
16 Brussels, Belgium

17 4- Gordon Center for Medical Imaging, Radiology Department, Massachusetts General  
18 Hospital, Harvard Medical School, MA 02114-1107, Boston, USA

19 5- Louvain Aging Brain Lab, Walloon Excellence in Life Sciences and Biotechnology (WELBIO),  
20 UCLouvain, Avenue E. Mounier 53, 1200 Brussels, Belgium.

21 Corresponding author: Frédéric Crevecoeur – [frederic.crevecoeur@uclouvain.be](mailto:frederic.crevecoeur@uclouvain.be)

22

23 Conflict of interest statement: The authors declare no competing financial interests.

24 Acknowledgments: Florence Blondiaux is a FRIA grantee of the Fonds de la Recherche Scientifique  
25 – FNRS (Be). The FNRS provided salary and research support for Bernard Hanseeuw under grants  
26 n° CCL40010417 and n° FRFS-WELBIO40010035. Frédéric Crevecoeur is supported by a grant from  
27 the FNRS under grant number 1.C.033.18.

28

29

30 **0. Abstract**

31           Essential tremor (ET) is a neurological disorder characterized by involuntary oscillations of  
32 the limbs. Previous studies have hypothesized that ET was a cerebellar disorder and reported  
33 impairments in motor adaptation. However, recent advances have highlighted that motor  
34 adaptation involved several components linked to anticipation and control, all dependent on  
35 cerebellum. We studied the contribution of both components in adaptation to better understand  
36 the adaptation impairments observed in ET from a behavioural perspective. To address this  
37 question, we investigated behavioural markers of adaptation in ET patients (n=20) and age-  
38 matched neurologically intact volunteers (n=20) in saccadic and upper limb adaptation tasks,  
39 probing compensation for target jumps and for velocity-dependent force fields, respectively. We  
40 found that both groups adapted their movements to the novel contexts, however, ET patients  
41 adapted to a lesser extent compared to neurologically intact volunteers. Importantly, components  
42 of the movement linked to anticipation were preserved in the ET group, whereas components  
43 linked to movement execution appeared responsible for the adaptation deficit in this group.  
44 Altogether, our results suggest that execution deficits may be a specific functional consequence of  
45 the alteration of neural pathways associated with ET.

46

47           New & Noteworthy: We tested Essential Tremor patients' adaptation abilities in classical  
48 tasks including saccadic adaptation to target jumps and reaching adaptation to force field  
49 disturbances. Patients' adaptation was present but impaired in both tasks. Interestingly, the  
50 deficits were mainly present during movement execution, while the anticipatory components of  
51 movements were similar to neurologically intact volunteers. These findings reinforce the  
52 hypothesis of a cerebellar origin for essential tremor and detail the motor adaptation impairments  
53 previously found in this disorder.

54

## 56 **1. Introduction**

57           Essential tremor (ET) is one of the most common movement disorders provoking  
58 involuntary oscillations of patients' limbs (1). Typical clinical features of ET are kinetic and intention  
59 tremors of limbs, particularly upper limbs and, to a lesser extent, head and trunk (2–4). To date,  
60 the pathophysiology of this neurological disorder is not fully understood, but some previous works  
61 have suggested a cerebellar origin (5). Neuroimaging studies reported abnormalities in the  
62 structure and connectivity of cerebellum as well as differences in the cerebello-thalamo-cortical  
63 loop (6–9). Postmortem studies also pointed towards alterations of cerebellar cells (10).  
64 Characterizing whether specific cerebellar functions are preserved or impaired in this condition is  
65 therefore important to better understand this disorder.

66           Crucial functions of cerebellum include movement control, state-estimation, and  
67 adaptation (11–13). The central nervous system cannot exactly access the state of the limbs  
68 (position, speed, etc.) due to the intrinsic delays in sensory feedback and to sensorimotor noise. As  
69 a result of this uncertainty, the brain must predict the next state that will be used to plan and  
70 control fast and accurate movements. The prediction is computed based on the delayed sensory  
71 feedback and an efferent copy of the motor command used in conjunction with prior knowledge of  
72 body and environmental dynamics. This operation of state estimation, which makes use of internal  
73 models, has been associated with cerebellum (14–17).

74           The ability to adapt motor patterns to novel environments rests on our ability to update the  
75 internal models used for estimation and control, thereby allowing for predictive compensation for  
76 sustained disturbance. It has been reported that adaptation depends on the integrity of  
77 cerebellum. The involvement of cerebellum in motor adaptation has been studied with a variety of  
78 movements, with non-human species (18, 19), as well as with cerebellar patients (20–22), who  
79 have shown deficits of adaptation in response to repeated perturbations. These results possibly  
80 reflect inaccurate internal models and a relative inability to update them in a way that counters the  
81 disturbance induced by the novel environment (11, 13).

82           Given the involvement of cerebellum in sensorimotor adaptation and its putative link with  
83 tremor, we set out to describe motor adaptation impairments in ET across two different tasks.  
84 Previous works reported that these patients were able to adapt to perturbations, but to a lesser  
85 extent than neurologically intact volunteers in force-field, visuomotor and prism adaptation tasks,  
86 as well as eyeblink conditioning (23–26). Considering that sensorimotor adaptation may involve  
87 multiple components (27), we aimed to expound this adaptation deficit using two tasks probing

88 visual and upper limb motor systems. In particular, we focused on the contributions of anticipation  
89 and movement execution on motor adaptation deficits. To do so, we studied adaptation in saccadic  
90 eye movements evoked by peri-saccadic target jumps, and upper limb reaching adaptation to  
91 velocity-dependent force fields as well as the correlation of adaptation performances in both tasks.  
92 We found that motor adaptation deficits observed in both tasks were due to the time course of  
93 movement execution while anticipatory compensation for the perturbation was comparable to the  
94 control group.

95 Our results support the hypothesis of a cerebellar origin for essential tremor but suggest a  
96 specific alteration of the pathways linked to the real-time motor execution across both visual and  
97 upper limb motor systems.

98

## 99 **2. Methods**

### 100 *Participants*

101 A total of 22 Essential Tremor (ET) patients and 20 neurologically intact (NI) volunteers  
102 participated in this study. All participants provided written informed consent following procedures  
103 approved by the Ethics Committee at the host institution (*Comité d'Éthique Hospitalo Facultaire*,  
104 UCLouvain, Belgium). A neurologist performed a clinical evaluation with the Fahn-Tolosa-Marin  
105 Tremor Rating Scale (FTM-TRS) (28) on all participants to evaluate the severity of the tremor. ET  
106 patients did not interrupt their medication before the assessment. We kept track of current  
107 medications and dosages (Supplementary Table 1). All but four ET participants took part in the two  
108 experiments. For the reaching experiment, one participant could not perform the task due to the  
109 amplitude of their hand tremor, another participant did not complete the task due to pre-existing  
110 shoulder condition. For the saccadic adaptation experiment, two other participants were excluded  
111 following technical limitations impeding calibration of the eye-tracking system. As a result, each  
112 population of ET patients was composed of 20 volunteers. Force sensors were defective for one ET  
113 participant, and another ET participant decided to stop the experiment a block earlier. We kept the  
114 data for the analyses and took into account the missing trials and the absence of force recordings.  
115 All NI volunteers participated in the two tasks, resulting in a group of 20 NI volunteers.

116 The FTM tremor rating scale was divided into three sections. Part A quantified the tremor  
117 amplitude of the limbs at rest, with posture holding, and during action. Part B quantified the action  
118 tremor of the upper limbs, particularly writing, drawing, and pouring liquids. Part C quantified the  
119 functional disability, evaluating patients' impairments in daily life activities (eating, drinking,  
120 working, etc.). We ignored this part filled by the participant due to the higher subjectivity of some

121 criteria and because our experiments assessed different tasks. Maximum scores for each section  
122 were respectively, 80, 32, and 28. Since this scale is not specific to ET evaluation, a low score in  
123 some items is expected like rest tremor, uncommon in ET.

124

## 125 *Tasks*

126 The study was composed of two experiments: a saccadic adaptation task (Figure 1&2) and a  
127 reaching adaptation task to a force field (Figure 3&4). During the saccadic adaptation task inspired  
128 from Xu-Wilson et al. (22), participants sat in a dark room on a height-adjustable chair in front of a  
129 screen. Head movements were restricted using a chin rest bar and forehead support. Eye  
130 movements were recorded using an Eyelink 1000 Tower-mounted eye tracker (SR Research,  
131 Ottawa, Canada) at a sampling rate of 1kHz, and stored for offline analyses. Participants gazed at  
132 the green targets (0.8 visual degrees wide) displayed on the screen. After a series of baseline trials  
133 containing a fixation target and a goal target, a jump of the goal target was introduced as a  
134 perturbation for the adaptation trials (Figure 1a&b). We divided the experiment into 7 blocks:  
135 oblique (30 trials), horizontal (30 trials), and five adaptation blocks (60 trials each). Coordinates are  
136 expressed in degrees of visual angle both for the horizontal and vertical component, with the  
137 center (0°,0°) being straight ahead of the participants.

138 During the oblique trials, a fixation target (F: (-10°,0°)) was projected on the left side of the  
139 screen. After a random wait time between 2 sec and 3 sec distributed uniformly, a new target was  
140 projected 20° away from the fixation target in the horizontal direction and 5° above the meridian  
141 vertically (T1: (10°,5°)). For the horizontal trials, the same fixation target (F) was used, and the final  
142 target was 20° away in the horizontal direction but aligned vertically (T1: (10°,0°)). We refer to the  
143 initial measurements of oblique and horizontal trials as *baseline* trials. The adaptation trials started  
144 with the same initial fixation target (F). A second target displayed 20° to the right appeared (T1:  
145 (10°,0°)), and participants were instructed to direct their gaze to the new target. As soon as the  
146 saccade was detected, the target jumped 5° away in the vertical direction (T2: (10°,5°)). The target  
147 T2 served as a fixation target for the next trial, the jump continued to be counterclockwise (F =  
148 (10°,5°); T1: (-10,5°); T2: (-10,0°)). See Figure 1a&b for a sketch of the different targets coordinates.  
149 The saccades were detected based on a horizontal velocity threshold of 150°/s computed online  
150 using backward 2<sup>nd</sup> order finite differences. Because of the perturbation, the saccade towards T1  
151 was followed by a corrective saccade towards T2. An inter trial time of 2.3sec was used in all cases.  
152 Participants took a short break between each block (15sec to 1min).

153 For the reaching adaptation task, participants sat on a height-adjustable chair in front of an  
154 End Point KINARM device (KINARM, Kingston, Ontario). They grabbed the handle of the robotic  
155 arm and performed reaching movements toward the target projected on the screen (Figure 3a). All  
156 participants performed the experiment with their right arm, independently of their laterality based  
157 on recent observation that adaptation on each side for the same task is very similar (29). The  
158 device recorded the participants' hand cursor position and forces applied to the handle. An  
159 occluder blocked the direct vision of the hand, but a hand-aligned cursor was always represented  
160 (white dot, radius 0.6 cm). The radius of the targets was 1.2 cm. A criterion on movement time was  
161 applied to encourage consistent velocities, but all movements crossing the target at least once and  
162 finishing within less than 3 cm from its center were kept for analyses. Good movement time ([600  
163 ms – 1500 ms]) was indicated by a green target at the end of the trial. If the participant was too  
164 slow, the target remained red and full. For movements too quick, the target switched to red and  
165 hollow. The experiment was composed of two trial types: null-field trials, and force field trials.  
166 During the null-field block (40 trials), participants were instructed to reach and stop at the  
167 displayed target. Two goal targets were used to avoid potential bias linked to the repetition of one  
168 target and to make the task less repetitive. The two goal targets and the start target formed an  
169 equilateral triangle. Targets centers were 10 cm apart. The start target, closest to the participant,  
170 was aligned with their elbow. For each trial, one of the two possible goal target was randomly  
171 selected and displayed on the screen. Each set was composed of the same number of trials  
172 towards each target. The adaptation blocks (4 blocks) featured trials with similar instructions but  
173 performed in the presence of a clockwise velocity-dependent curl field applied throughout the  
174 whole movement. The force field was defined as followed:  $f_x = 15 \dot{y}$  and  $f_y = -15 \dot{x}$  (N). Each  
175 block was composed of 66 trials: 30 trials towards each target with the force field, and 3 catch  
176 trials per target during which the force field was unpredictably turned off. The trials were  
177 presented in random order. The inter-trial time was 1sec. Participants were encouraged to take  
178 short breaks between the blocks to reduce fatigue (15 sec to 1 min).

179

### 180 *Data Analysis*

181 Raw measurements of eye position were filtered with a dual-pass 4<sup>th</sup> order low pass  
182 Butterworth filter with a cut-off frequency of 50 Hz. Eye velocity was computed based on position  
183 signals using 4<sup>th</sup> order finite differences. The beginning and end of each saccade were defined  
184 using a threshold on the horizontal eye velocity of 16°/s for at least 10 ms. Additional criteria for  
185 saccade inclusion were: (1) its duration, within 50 to 200 ms, (2) its peak velocity, above 100°/s,

186 and (3) a minimum amplitude of 10°, corresponding to one-half of the instructed horizontal  
187 displacement. These inclusion/exclusion criteria were adapted from (22). On average, NI  
188 volunteers had 11.7% of their trials excluded (min: 3.9%, max: 38.9%), ET patients 14.7% excluded  
189 (min: 3.9%, max: 31.4%). Non-detected saccades were mainly due to blinks and fatigue leading to  
190 poor detection of the pupil by the eye-tracking system. The mean velocity was computed on a  
191 40ms window, centered around the trial's peak velocity. The curvature of saccades was  
192 approximated using the same method as Chen-Harris and colleagues (30). Each saccade was  
193 divided into 4 equal segments along the horizontal direction, the slope of the line extending the  
194 end of each segment was computed and was referred to as S1-S4 (see Figure 2c-g). The timing of  
195 each segment was in average 21.7ms, 11.8ms, 13.2ms and 28.5ms. After observing no qualitative  
196 differences between the left and right saccades, adaptation trials in both directions were  
197 combined for analyses.

198 For the reaching adaptation task, the data was filtered using a dual-pass 6<sup>th</sup> order low pass  
199 Butterworth filter with a cut-off frequency of 25 Hz. Movement onset and end were defined using  
200 a speed threshold of 3cm/s. Movements were included in the dataset if their duration was above  
201 300ms, crossed at least once the target, and ended less than 3cm from the target center. Based on  
202 this criterion, we excluded in average 1.1% of the trials for NI participants (min: 0.3%, max: 2.3%)  
203 and 4.9% of the trials for ET patients (min: 0%, max: 21.1%). Adaptation was quantified using  
204 Pearson's correlation between the force orthogonal to straight path measured at the interface  
205 between the hand and the robot handle (measured force), and the force field commanded by the  
206 robot and extracted offline based on velocity signals of each trial (commanded force). Intuitively, if  
207 the measured force and the commanded force are equal and opposite, one expects high values of  
208 correlation between these signals. In contrast, a lack of knowledge of the force field producing only  
209 approximate or poorly tuned compensation for the perturbation should yield lower correlation  
210 values. It was also verified empirically that this metric was indeed sensitive to adaptation in the  
211 same setup and task (31). Initial angles, between the hand path and the straight line connecting  
212 the two targets, were computed at 200ms after movement initiation, with a counter-clockwise  
213 angle being defined as positive. We verified that there was no qualitative difference between the  
214 two targets, thus movements were remapped and combined for all analyses. We used a constant  
215 bin width of 8 trials for illustration purposes to show the effect of the perturbations.

216

217 *Statistical Analysis*

218 In both experiments, Student's t-tests were used to compare performances between  
219 groups during baseline condition (endpoint and maximum velocity of the saccade, movement  
220 duration, and path length of the reaching movement) and for the initial angles from catch trials in  
221 the reaching adaptation task. T-tests were also used to compare average group age. Adaptation  
222 was evaluated using two techniques: exponential fits and Linear Mixed Effects (LME) models. A  
223 standard exponential model of adaptation was fitted on group average and 95% confidence  
224 intervals of each parameter were compared between ET and NI. The parameter  $a$  corresponds to  
225 the final offset to which the exponential curve converges,  $b$  is the amplitude of adaptation which  
226 therefore impacts the starting point of the curve, and  $c$  to the learning rate. The variable  $i$  was the  
227 trial number. The exponential fit was as follows:

$$228 \quad y = a + b * e^{-c*i} . \quad (1)$$

229

230 Because the exponential fits were not significant in all cases, we also used linear mixed  
231 models to assess the evolution of the dependent variables across trials and group while taking  
232 inter-individual variance as a random factor. More precisely, LME models were fitted with factors  
233 *Trial Number (i)* and *Group* (2 level factor) as fixed predictors, and a random intercept to capture  
234 idiosyncrasy. LME and exponential fits were used for vertical end-point, vertical velocity, and  
235 saccades slopes in the first experiment, and maximum perturbation forces, normalized deviation,  
236 initial angle, and forces correlations in the second experiment. For each dependent variable the  
237 formulae of LME was:

238

$$239 \quad Y_{ij} = \beta_0 + \beta_1 * i + \beta_2 * Group + \beta_3 * Group * i + b_j + \epsilon_{i,j} , \quad (2)$$

240

241 where  $Y_{ij}$  represents the dependent variable of trial number  $i$  from participant  $j$ ,  $\beta_i$  are the  
242 coefficient of the fixed predictors including trial number, group (control or ET), and interaction  
243 between them, and  $b_j$  is the random intercept for participant  $j$ , and  $\epsilon_{i,j}$  is the residual.

244 To measure the variability of the movements, we investigated several bins across the movement  
245 and kept the bin with the highest variability which corresponded to 20ms around the midpoint  
246 between peak velocity and target crossing for the reaching adaptation and 20ms around the  
247 midpoint between peak velocity and movement end for the saccadic adaptation. Variability of each  
248 person was computed using their movement in each block. We compared variability of participants  
249 using Wilcoxon rank-sum tests. For the unpaired comparisons between groups, due to the limited  
250 number of participants and the inherent variability of our populations we defined the significance

251 threshold at 0.05. This includes Spearman's and Pearson's correlations, Wilcoxon rank-sum tests  
252 and Student's t-test. Concerning the LME, where all trials are considered we expect increased  
253 statistical power and therefore assessed the significance of each effect using an F-test and a  
254 significance threshold of 0.005 (32, 33).

255 Finally, a linear support vector machine classifier was trained on the final performances of  
256 each participant in a 2-dimensional space that contained the learning indices that exhibited strong  
257 differences across trials and groups. The purpose of the classification technique was to quantify  
258 the overlap between the two groups in this two-dimensional space, however the accuracy of the  
259 model was still assessed based on leave-one-out cross-validation. In addition to quantifying the  
260 overlap between the distributions, the support vector machine was also used to illustrate that the  
261 boundary between the two groups separated the plane into overall better or worse performances  
262 in the two groups. All analyses were performed offline with Matlab 2020b. The data will be  
263 available in Zenodo following the publication of the article.

264

### 265 **3. Results**

#### 266 *Experiment 1: Saccadic Adaptation*

267 We instructed participants to perform visually guided saccades to a target projected on a  
268 screen. The time course of a trial followed standard protocols of saccadic adaptation (22, 30): after  
269 an initial fixation delay, the target was projected, and participants initiated a saccade (Figure  
270 1a&b). During movement, the goal target jumped vertically, inducing a terminal error that was  
271 gradually reduced as adaptation progressed. The experiment started with baseline trials, during  
272 which the target did not jump (see Methods). A total of 40 volunteers took part to this experiment,  
273 20 Essential Tremor (ET) patients (14 F, 6 M) and 20 neurologically intact (NI) volunteers (14 F, 6  
274 M). There was no significant difference in age between ET patients (M = 58.6, SD = 15.4) and NI  
275 volunteers (M=56.8, SD = 12.4); (t-test;  $t_{38}=-0.4013$ ,  $p= 0.69$ ). We assessed tremor severity in all  
276 participants using the Fahn-Tolosa-Marin Tremor Rating Scale (FTM-TRS). ET patients obtained an  
277 average score of  $8.8 \pm 5$  (mean  $\pm$  SD) points in part A assessing tremor amplitude and  $14.6 \pm 7.6$   
278 points for part B which assesses drawings and pouring (part B). The average score of NI  
279 participants was  $1 \pm 1.3$  (part A) and  $1.5 \pm 1.7$  (part B).

280

281

282

[Insert Fig1 here]

283

284

**Figure 1** Schematic representation of the saccadic adaptation protocol design (**a,b**) & behavior in saccadic adaptation task (**c,d**). **a** Time course of a trial in the saccadic -adaptation task. A: Participants (n=40) were asked to

285 perform saccades to gaze at a target visible on the screen. The experiment was divided into 3 trial types: oblique  
286 saccades, horizontal saccades, and adaptation saccades. Each trial began with a fixation target (F), followed by the  
287 appearance of the goal target (T1) after a random delay. Locations are indicated in visual degrees. During adaptation  
288 trials, the goal target was shifted by 5 degrees (T2). These trials occurred in two directions, to the right (black) and the  
289 left (grey). Target jump was counterclockwise. The dashed lines depict the axes centered straight ahead. **B** Target  
290 sequence from an adaptation trial. Arrows indicate when a saccade was initiated. Target jump (T1 to T2) occurs when  
291 the saccade is initiated. At the end of the trial, T2 served as fixation for the next trial (grey in 1A). **c** (Left) Group  
292 average of participants' eye trajectories averaged over the oblique and horizontal blocks. Grey dots represent the  
293 targets. (Right) Vertical end point and mean vertical velocity of saccades, across all trials, and averaged for the two  
294 groups. Error bars represent the SEM. Grey dots represent individual datapoints. **D** (Left) Saccades averaged over the  
295 first and last 10 trials to highlight differences between early and late adaptation phases. (Right) Average velocity traces  
296 are plotted for the horizontal and vertical components. Thin traces correspond to the horizontal baseline trials. Shaded  
297 areas represent the SEM.

300 The average eye trajectories of the baseline phase of the experiment are depicted in Figure  
301 1c, left panel. No significant differences of vertical (t-tests; oblique:  $t_{38}=0.47$ ,  $p=0.64$ ; horizontal:  
302  $t_{38}=0.55$ ,  $p=0.58$ ) and horizontal (t-tests; oblique:  $t_{38}=0.23$ ,  $p=0.82$ ; horizontal:  $t_{38}=0.79$ ,  $p=0.43$ )  
303 end-point were observed between the two participants groups during these baseline trials.  
304 Likewise, average vertical (t-tests; oblique:  $t_{38}=0.39$ ,  $p=0.7$ ; horizontal:  $t_{38}=1.04$ ,  $p=0.31$ ) and  
305 horizontal (t-tests; oblique:  $t_{38}=-0.19$ ,  $p=0.85$ ; horizontal:  $t_{38}=-0.28$ ,  $p=0.78$ ) velocities were similar  
306 across the two groups. Mean velocity was computed on a 40ms window centered on the trial's  
307 peak velocity. No statistical differences were observed regarding the fixation prior to the saccade,  
308 which was assessed by comparing averaged position and velocity across a 100ms window prior  
309 saccade initiation.

310 During the adaptation phase of the experiment, the target jumped vertically (5 visual  
311 degrees up/down) depending on the saccade direction (right/left respectively). The perturbation  
312 resulted in an endpoint error corrected by a second saccade. Both groups adapted their saccades  
313 to the target jump by increasing the vertical endpoint coordinate of the first saccade, but the  
314 extent of adaptation was significantly smaller for ET patients. The average eye trajectories at the  
315 beginning and the end of adaptation trials are plotted for each participant in Figure 1d. First, the  
316 vertical end-point of saccade increased with trial repetitions to reach an average of  $2.06^\circ$  (visual  
317 degrees) for NI participants, and only  $1.83^\circ$  for ET patients as can be seen in Figure 2a. Exponential  
318 fits were generally non-significant for the saccadic adaptation task (except for the 3<sup>rd</sup> slope), we  
319 therefore only present LME analyses for this task. A linear mixed-effect (LME) model revealed a  
320 significant main effect of the trial ( $F_{(10,356)} = 24.20$ ,  $p < 10^{-4}$ ), no effect of the group (NI or ET) on the  
321 vertical end point was observed ( $F_{(38)} = -0.44$ ,  $p=0.66$ ) but there was a clear interaction effect  
322 between these two factors with a negative coefficient ( $F_{(10,356)} = -5.22$ ,  $p < 10^{-4}$ ). This model shows  
323 that even if both groups started at the same level (no main effect, thus no offset on average) ET

324 patients adapted at a lower rate to the perturbation than neurologically intact volunteers  
325 (interaction effect). The mean vertical velocity increased with trials for both groups, but with a  
326 smaller increase for the ET group (Figure 2b, LME; Trial :  $F_{(10,356)} = 0.07$ ,  $P < 10^{-4}$  ; Group:  $F_{(38)} = -2.16$ ,  
327  $P = 0.51$ ; Group-by-Trial :  $F_{(10,356)} = -6.14$ ,  $P < 10^{-4}$ ). Participants performed a corrective saccade, in  
328 order to reach the final target T2. The amplitude of this saccade decreased with trial repetition, in  
329 accordance with the increase in the vertical endpoint coordinate of the first saccade. Similar to the  
330 first saccade, there was no group effect for the amplitude of the corrective saccade, but there was  
331 a significant interaction between the group and trial number, reflecting that ET patients adapted  
332 less to the perturbation (LME: Trial:  $F_{(9497)} = -17.4$ ,  $P < 10^{-4}$ ; Group:  $F_{(38)} = 0.29$ ,  $P = 0.78$  ; Group: Trial:  
333  $F_{(9255)} = 3.89$ ,  $P < 10^{-3}$ ).

334

335 [Insert Fig2 here]

336 **Figure 2 – Participants' behaviour during the saccadic adaptation task**

337 ET patients showed reduced saccadic adaptation **a, b**, Evolution of the vertical end point (a) and peak vertical velocity  
338 (b) averaged over each group. Shading indicates SEM. **c**, The curvature was approximated by dividing saccade into 4  
339 segments along the horizontal axis and by computing the slope of each segment (labeled S1 – S4). **d-g**, Evolution of the  
340 segment slopes with adaptation. **a,b,d-g**, grey area: Behavior in the horizontal baseline trials, error bars depicts the  
341 SEM.

342

343 Previous studies on saccadic adaptation (22, 30) reported a specific pattern in the evolution  
344 of saccades curvature, differentiating adapted saccades from oblique saccades with the same  
345 amplitude. Using the same technique, we approximated the saccade curvature by dividing the  
346 saccade into four equal segments along the horizontal axis and analyzed the evolution of the slope  
347 of each segment (S1-S4) (Figure 2c-g, see Methods). The differences between the slopes of  
348 segments is a proxy of the curvature since highly curved movements should display large variations  
349 in consecutive slopes. We observed an altered adaptation pattern in ET patients. The LME model  
350 revealed a significant effect of the trial and of the interaction between group and trial for all  
351 segments but the first one (LME; S1: Trial:  $F_{(10,356)} = 8.41$ ,  $p < 10^{-4}$  ; Group:  $F_{(38)} = -0.25$ ,  $p = 0.8$ ; Group-  
352 by-Trial:  $F_{(10,356)} = -1.25$ ,  $p = 0.21$ ; For S2-S4 Trial:  $F_{(10,356)} > 15.01$ ,  $p < 10^{-4}$  ; Group:  $F_{(38)} > 0.09$ ,  $p > 0.24$ ;  
353 Group-by-Trial:  $F_{(10,356)} < -2.88$ ,  $p < 0.004$ ). Differences between NI and ET participants were maximal  
354 during S2 and S3. Interestingly, the fact that the first segment of the saccade was similar across  
355 groups suggested the preservation of the initial component of saccadic adaptation -which could be  
356 seen as a proxy of anticipatory compensation-, whereas differences in S2 and S3 indicated  
357 impairment in the time course of saccadic execution supported by internal feedback. We studied  
358 whether any relationship existed between anticipation and real-time execution performances. For  
359 the patient group, we computed the correlation between the slope of the first segment and the

360 end point, the correlation coefficient was 0.5 with a p-value of 0.03 (Spearman correlation). This  
361 relationship was expected as reported in Chen-Harris study where S1 was responsible of 75% of  
362 the total adaptation (30).

363 Finally, we compared the variability of participants' behaviour during the baseline blocks,  
364 and during the last trial of adaptation to observe participants' consistency during the task. We only  
365 report the results for the horizontal position, but similar results were observed for the other  
366 metrics (including vertical position as well as velocities in each direction). The variability was the  
367 most important towards the end of the movement, midway between peak horizontal velocity and  
368 the end of the movement. For the horizontal, oblique and last block of adaptation, patients were  
369 respectively 28.8 %, 27.6% and 18.3% significantly more variable than controls (Wilcoxon rank-  
370 sum test:  $T > 489$ ,  $z > 2.12$ ,  $p < 0.03$ ). This variability was not correlated with the FTM-TRS score nor  
371 the task performance.

### 372 *Experiment 2: Adaptation of reaching movements to a force field*

373 For this experiment, we tested 20 ET patients (15 F, 5 M) and 20 NI participants (14 F, 6 M).  
374 The NI group was identical to the saccadic adaptation experiment, whereas the ET group involved  
375 18 participants that were also tested in the saccadic adaptation task and 2 new participants. As for  
376 the saccadic adaptation task, we verified that there was no significant difference in age between  
377 the two groups (ET patients : M: 57.7, SD: 16.1, t-test:  $t_{38} = -0.19$ ,  $p = 0.85$ ). ET patients obtained an  
378 FTM-TRS score of  $9 \pm 4.8$  for part A (tremor amplitude) and  $13.7 \pm 6.5$  for part B  
379 (drawings/pouring).

380 Participants first performed 40 movements moving the robotic handle of an instrumented  
381 device (KINARM, Kingston, ON) in a null field. These movements were used as control trials to  
382 measure differences between the two groups when no perturbation occurred (Figure 3a-d). We  
383 decomposed the trials into a reaching and a stabilization phase that were defined based on the  
384 time at which participant's hand crossed the target for the first time. The last movement of each  
385 participant in this field is depicted in grey in Figure 3f. The reaching phase was exempt of  
386 oscillations: movement duration and path length were similar for both groups (Figure 3e, t-test;  
387 Movement duration:  $t_{38} = -0.16$ ,  $p = 0.87$ ; Path length:  $t_{38} = -0.66$ ,  $p = 0.51$ ). The stabilization phase was,  
388 however, directly impacted by the tremor with longer movement duration and path length (Figure  
389 3e, t-test; Movement duration:  $t_{38} = -2.95$ ,  $p = 0.005$ ; Path length:  $t_{38} = -3.3$ ,  $p = 0.002$ ). Initial  
390 assumptions were not made regarding differences between reaching and stabilization.  
391 Nevertheless for the subsequent analyses, we focused on the reaching phase of the movement –

392 similar across groups in the absence of perturbation – as adaptation indices taken from this  
393 window would likely not be directly affected by the tremor.

394

395 [Insert Fig3 here]

396 **Figure 3** Schematic representation of the upper limb adaptation protocol design (a-d) & Participants behavior  
397 during the reaching adaptation task (e,f). **A**, Participants (n=40) were asked to perform reaching movement to one of  
398 two goal targets displayed on the screen 10 cm away from the start target with hand-aligned cursor. Direct view of the  
399 limb was blocked. The timing of the movement was constrained, the go cue was given by the filling of the goal target.  
400 Visual feedback about movement timing was provided (see Methods). **B**, Parameters extracted from individual traces:  
401 the initial angle was defined as the angle between the straight line connecting the two targets and the hand position at  
402 200ms. Counter-clockwise angle is defined as positive. Maximum deviation was computed between hand path and the  
403 straight line connecting the targets. **C**, Lateral Forces applied by participant on the handle (solid traces) and applied by  
404 the robot (grey traces) for an exemplar participant from the control group. Top and bottom panels illustrate the  
405 difference between early and late phases of the adaptation blocks. It can be observed that the applied force was closer  
406 to the perturbation force at the end of the adaptation phase. **D**, Time course of the protocol: 20 baseline trials towards  
407 each target (no force field). Adaptation trials were composed of 120 trials in each direction perturbed by a velocity  
408 dependent clockwise curl force field. Randomly interleaved catch trials (no force field) were included during the  
409 adaptation blocks. Target presentation order was randomized for each block. **E**, Movements were divided into reaching  
410 and stabilization. The end of reaching corresponded to the time at which the cursor crossed the target boundary.  
411 Significant differences between the two groups in movement duration and hand path lengths were observed only  
412 during the stabilization part. Error bars represent SEM. Note the modified scale for the stabilization measures. **F**,  
413 Participants' hand paths during the first (top) and last (bottom) force field trial. The differences between the trials  
414 illustrate adaptation. Grey traces correspond to the last baseline trial of each participant.

415

416 When participants were exposed to the force field for the first time, they all  
417 experienced large lateral hand deviations (Figure 3f). After a few trials, they quickly adapted their  
418 movements to the perturbation, and a reduction of the deviation relative to a straight line was  
419 observed: the path length decreased and the forces applied by the participant paralleled the one  
420 applied by the robot, a good compensation being the opposite of the perturbation (Figure 3c).

421 Similar to the saccadic adaptation task, both groups showed an adaptation of their  
422 movements to the force field, however, this adaptation was reduced for ET patients. The ET  
423 patients were slower in the task (Figure 4a&b; Movement duration – LME: Trial:  $F_{(9255)} = -2.73$ ,  
424  $P < 10^{-2}$ ; Group:  $F_{(38)} = 2.19$ ,  $P = 0.03$ ; Group: Trial:  $F_{(9255)} = -3.6$ ,  $P < 10^{-3}$ ). This resulted in a significantly  
425 smaller perturbation (Figure 4c; LME: Trial:  $F_{(9255)} = -13.11$ ,  $P < 10^{-4}$ ; Group:  $F_{(38)} = -1.65$ ,  $P = 0.11$ ;  
426 Group: Trial:  $F_{(9255)} = 6.62$ ,  $P < 10^{-4}$ ). To account for this difference, the maximum deviation measured  
427 during each trial (Figure 4d) was normalized by the maximum perturbation force during the trial.  
428 The normalized deviation (Figure 4e) was significantly higher in the ET group as revealed by the  
429 exponential fits, where all fitted parameters revealed reduced adaptation in the ET population  
430 (Figure 4e, asymptote (a) ET:  $a = 0.33$  (95% CI: 0.32-0.34),  $P < 10^{-4}$ , NI:  $a = 0.23$  (0.22-0.24),  $P < 10^{-4}$ ,  
431 amplitude (b) ET:  $b = 0.30$  (0.24-0.37),  $P < 10^{-4}$ , NI:  $b = 0.21$  (0.19-0.23),  $P < 10^{-4}$  and learning rate ET:  
432  $c = 0.10$  (0.07-0.14),  $P < 10^{-4}$ , NI:  $c = 0.02$  (0.015-0.025),  $P < 10^{-4}$ ). LME confirmed these results with a

433 significant interaction between the group and the trial number (Figure 4e; LME: Trial:  $F_{(9255)} =$   
434  $19.78, P < 10^{-4}$ ; Group:  $F_{(38)} = 0.91, P = 0.37$ ; Group: Trial:  $F_{(9256)} = 5.60, P < 10^{-4}$ ).

435

436

[Insert Fig4 here]

437

438

439

440

441

442

443

444

445

446

447

**Figure 4** – *Participants' adaptation during the reaching task* **a**, Maximum forward velocity during the adaptation trials, used to compute the lateral perturbation. **b**, Movement duration during the reaching phase **c**, Maximum lateral perturbation received by the participants during the adaptation trials. Averaged over each group. **d**, Maximum hand deviation observed during force field trials. **e**, Maximum lateral deviation, normalized by the averaged force received during reaching. **f**, Initial angle between the hand and the line connecting the start-target centers at 200ms after movement initiation. **g**, Cumulative distribution of the initial angle during the catch trials for the ET and NI participants. **h**, Trial by trial correlation between the force field applied by the robot and the forces applied by the participant. Averaged over participants of each group. **a-f, h**, Shaded areas represent the SEM, grey area: average behavior in the baseline trials, error bars depicts the SEM. **e,f,h**: Significant exponential fits.

448

449

450

451

452

453

454

455

456

457

458

459

460

461

462

The initial reach angle is defined as the angle between the position of the hand at 200ms and the straight line connecting the home and the goal target (Figure 3b). It is a proxy of participants' anticipation of the perturbation as the earliest modulation of motor commands within movement was previously reported at ~250ms after movement onset (27, 31). It suggests that movement parameters prior to this time must be linked to anticipation. It is expected that the force field produces negative values of initial angles early in the adaptation phase, with gradual changes towards 0 as adaptation progresses. Exponential fits reported similar learning rates and amplitude for both groups but a significant difference in the asymptote (ET:  $a = -2.5$  (95% CI:  $-2.8, -2.3$ ),  $P < 10^{-4}$ , NI:  $a = -1.7$  ( $-1.9, -1.5$ ),  $P < 10^{-4}$ ). Mixed models analyses reported a small difference in learning rate for the initial angles (Figure 4f), suggesting that both groups had slight differences in initial angles (LME: Trial:  $F_{(9255)} = 5.35, P < 10^{-4}$ ; Group:  $F_{(38)} = 0.03, P = 0.98$ ; Group: Trial:  $F_{(9255)} = -3.40, P < 10^{-3}$ ). However, no difference in initial angles was observed during the catch trials (Figure 4g; *t*-test;  $t_{38} = 0.83, p = 0.41$ ). Similarly, the distributions were not significantly different (Kolmogorov-Smirnov test:  $D(38) = 0.2, p = 0.77$ ). Overall, these results reflected no significant differences between the two groups in anticipating the perturbation.

463

464

465

466

467

468

469

470

In contrast, the compensation for the force field during movement was more strongly impacted. We computed the correlation between the perturbation force and the force measured at the handle, a high correlation highlighting a good compensation for the force field (31). We found an increase across trials for both groups, while remaining significantly smaller for ET patients than for NI participants (Figure 4h). Exponential fits reported a difference of asymptote (ET:  $a = 0.81$  ( $0.8-0.82$ ), NI:  $a = 0.86$  ( $0.85-0.87$ )) and no significant differences in amplitude or learning rate. This result was also confirmed by LME models (Trial:  $F_{(9020)} = 20.41, P < 10^{-4}$ ; Group:  $F_{(37)} = -2.41, P = 0.021$ ; Group: Trial:  $F_{(9020)} = 0.74, P = 0.46$ ). Interestingly, the reaching adaptation experiment revealed

471 impairments qualitatively similar to the saccadic adaptation task: first, ET patients were able to  
472 adapt, but they exhibited reduced adaptation in comparison with the control group. In both  
473 experiments, it appeared that the aspects linked to anticipation were preserved (S1 for the  
474 saccadic adaptation, the catch trials initial angles for the reaching task), whereas the metric closely  
475 linked to online execution exhibited a reduced compensation for the perturbation (S2 and S3 for  
476 the first task, and the correlations computed on continuous force traces for the reaching task). We  
477 did not find any significant correlation between the initial angle and the correlations (Spearman's  
478 correlation for the patient group; 0.38,  $p=0.12$ ), suggesting an absence of interaction between  
479 both adaptation mechanisms.

480 We also compared participants' variability during the baseline block and the last block of  
481 adaptation. Variability peaked close to the end of the movement, midway between peak forward  
482 velocity and target crossing. During the baseline and the last block of adaptation, for the lateral  
483 velocity, ET patients were in average 51.4% and 49.6% significantly more variable than NI  
484 participants (Wilcoxon rank-sum test:  $T>519$ ,  $z>2.93$ ,  $p<0.003$ ). This variability was not correlated  
485 with the FTM-TRS score nor the task performance. Similar results were observed for the lateral and  
486 forward position and velocity with a difference for the Spearman's correlations in the forward  
487 position where the variability positively correlated with the tremor score (Spearman correlation;  
488 baseline: 0.54,  $p=0.01$ , last block of adaptation: 0.45,  $p=0.046$ ) and negatively with task  
489 performances during the baseline block (Spearman correlation; baseline:  $-0.75$ ,  $p<10^{-3}$ , last block  
490 of adaptation:  $-0.46$ ,  $p=0.057$ ). We also observed trends in two other conditions for both  
491 comparisons ( $p<0.10$ ).

492

#### 493 *Correlations between task performances and FTM-TRS scores*

494 We investigated the correlation of tremor severity with the impairment for each task.  
495 Despite ET patients' significant impairment of saccadic adaptation, the FTM-TRS score (part A+B)  
496 was not correlated with the vertical end-point at the end of the adaptation (Figure 5a; Pearson's  
497 correlation = 0.11,  $p = 0.65$ ). Concerning the force field adaptation task, a trend between the  
498 correlation of forces and the FTM-TRS score was observed (Figure 5b; Pearson's correlation =  $-0.47$ ,  
499  $p=0.047$ ), suggesting that most affected ET patients were also those showing the larger  
500 impairment in reaching adaptation. It is clear that one participant with lowest task performance  
501 score both epitomizes and drives this effect. On the one hand, there was no anomaly with their  
502 data meaning that the result is likely valid. On the other hand, the correlation diminished to  $-0.40$

503 with a p-value of 0.11 after removing this data point. In any case, additional data may be necessary  
504 to address the robustness of this relationship.

505 [Insert Fig5 here]

**Figure 5** – *Correlation between performance and tremor score*

**a, b**, Relationship between the score obtained during late adaptation (**a**, Saccadic adaptation, **b**, Force field adaptation) and the Tremor Score measured via the FTM TRS scale (Part A+B). Each dot represents the average score obtained over the last 10% trials. **C**, Relationship between the performances in the two tasks for each participant. Color gradient represents the FTM TRS Score. The separation between the two groups was computed by training a linear support vector machine to discriminate populations based on the scores obtained in each task (accuracy: 67.6%). Red circle highlight a misclassification error for a less severely affected ET participant.

506 Finally, we sought to quantify the differences between the two-dimensional distributions of  
507 adaptation indices to measure the overlap across NI and patient's groups. We used a linear  
508 support vector machine, trained on the vertical end-point error and the continuous correlations, to  
509 visualize which task performances regions were associated with each group and quantify the  
510 overlap between the two populations taking two-dimensional linear separation in the space of  
511 adaptation indices. The classifier separated our performance space into reduced performances in  
512 both tasks for ET patients and higher performances in both tasks for NI volunteers, as shown in  
513 Figure 5c. In this dataset, participants classified in the blue region had an average FTM-TRS score of  
514 7.1 points; participants classified in the orange region had an average score of 18.6 points. The  
515 support vector machine leave-one-out cross-validation accuracy was 67.6%. Classification errors  
516 mainly occurred for patients with a lower FTM-TRS score. Misclassifications happened more  
517 frequently for ET patients with lower FTM-TRS scores, closer to NI participants' scores. An example  
518 of misclassification for a less severely affected ET patient is highlighted on Figure 5c.

519

#### 520 **4. Discussion**

521 Our study aimed to better understand the origin of the sensorimotor adaptation deficits  
522 previously reported in ET patients. To do so, we selected standard reaching and saccadic  
523 adaptation tasks known to be altered in patients with cerebellar deficits. As expected, ET patients  
524 experienced a deficit of adaptation in both tasks when compared with the control group.  
525 Importantly, our study revealed that the aspects linked to the anticipation of the perturbation,  
526 namely the initial saccade slope, the catch trials, and the initial reach angles, clearly evolved across  
527 trials and were intact for ET patients. In contrast the deficits seemed to be linked to markers of  
528 online control (intermediate saccade slopes and correlations in the reaching task).

529 Our results are consistent with previous adaptation studies performed with ET patients in  
530 various tasks (23–26). Here we reproduced the results of Chen et al. (23), and added to this line of

531 evidence that the impairment in adaptation in ET patients may reflect a general sensorimotor  
532 deficit as it also impacts adaptation of saccades despite the absence of ET symptoms in  
533 unperturbed saccades (34, 35).

534 Although a linear correlation was not observed between the tremor score and the  
535 performance in the saccadic adaptation task, a trend was observed indicating that higher tremor  
536 score were related to lower performance in the force field adaptation task. This result might be  
537 explained by the fact that the FTM-TRS scale mostly evaluates upper limb sensorimotor function  
538 and tremor, whereas eye movements are not included or evaluated in this clinical scale. The  
539 overall tendency was an ordering of the patient's group in the region of the space of parameters  
540 used to quantify adaptation corresponding to lower performances in both tasks.

541 A previous study reported an interaction between noise and adaptation performances (36).  
542 They reported a decreased adaptation rate when execution noise (noise originating from the  
543 sensorimotor pathway) was more important and increased adaptation rate when planning noise  
544 was more important. A parallel can be made here between execution noise and the increased  
545 variability observed in the population with ET. Interestingly, a negative trend was observed  
546 between variability and task performances and a positive trend between variability and tremor  
547 score for half of the metrics studied in the reaching adaptation task.

548 Our study is not without limitation but they may not have a strong impact on our  
549 interpretations. First, participants did not stop their medications before the evaluation, which may  
550 influence the FTM-TRS score. Our analyses of the correlations between performance and the  
551 tremor score were computed based on this score, and might therefore suffer from the  
552 heterogeneity of patients and treatments. Severely affected patients with efficient treatments  
553 might have a lower tremor score than less severely affected patients and therefore have an impact  
554 on the correlations computed. Accounting for the medication was however difficult due to the  
555 variety of treatments and dosages taken by the participants. Studying sensorimotor deficits while  
556 taking medication into account is likely a challenge for prospective studies. Besides the  
557 heterogeneity inherent with clinical population and the diversity of treatments, our conclusions  
558 are still supported by the fact that the components of motor control prior to the adaptation tasks  
559 were similar across groups. Another point of attention concerns the performance of our classifier,  
560 which requires validation and should not be hastily generalized. The classifier was used here to  
561 quantify the overlap between two distributions, and not to perform prediction on unseen data.  
562 The performance of such an approach must be validated with larger datasets before becoming a  
563 candidate test to improve the diagnosis of ET. Finally, previous work has reported the existence of

564 cognitive or explicit strategies during adaptation to force fields accounting for a fraction of force  
565 produced against a force field (37). It is clear that the initial movement angle could be composed  
566 of an explicit component, however it was likely similar across groups and our data do not allow us  
567 to isolate it. In addition, the main deficit again was linked to movement control which is difficult to  
568 relate to a cognitive bias or strategy in both tasks. We believe that quantifying the contribution of  
569 explicit components in ET is an interesting topic for follow-up studies.

570 In contrast with cerebellar ataxia, patients who showed dramatic impairments and almost  
571 complete absence of adaptation in the tasks performed in this present study, ET patients showed  
572 only reduced adaptation in both tasks (20, 22). When comparing the results of the control group  
573 obtained by Xu-Wilson et al. with our control group, it must be noted that adaptation in this study  
574 appears to be slightly reduced. This difference could be potentially attributed to variations in the  
575 experimental setup and protocols. Our motivation to conduct the present study was to parse out  
576 potential cerebellar deficits in ET patients. However, it is important to keep in mind that even if  
577 cerebellum seems to be involved, it does not exclude other causes. A clear difficulty in  
578 documenting these cerebellar deficits was that cerebellum has been associated with a wide range  
579 of sensorimotor functions, including motor adaptation and control (18–22). A common ground  
580 between adaptation and control is the use of internal models that have been also associated with  
581 cerebellum (11–13). It is widely assumed that the brain uses these internal models to produce an  
582 estimation of the next state based on the current state estimate and the sensory feedback. This  
583 estimation is required to perform fast and accurate movements in an unpredictable environment  
584 despite sensorimotor noise and delayed sensory feedback. Online monitoring of the movement  
585 and corrections inflight linked to cerebellar mechanisms was shown in saccadic eye movements  
586 (38–42), as well as reaching movements (17). It is therefore possible that internal models for  
587 control hosted in cerebellum would be responsible for tremor and for reduced online  
588 compensation in adaptation tasks. Such internal models can take several forms, including aspects  
589 linked to sensorimotor coordination, as well as operations linked to timing representations (43–  
590 46). In this regard, it is known that oscillations, explaining the low frequency components of ET  
591 tremor, can arise in a system that incorrectly compensates for sensorimotor delays (47, 48). Thus,  
592 we suggest that tremor arises from incorrect internal models in cerebellum likely associated with  
593 delay compensation, producing the well documented oscillations and deficits in online control.

594 The possible dissociation between anticipation and online control is important for  
595 interpreting ET disorders, and also potentially on the underlying dysfunction of the cerebello-  
596 thalamo-cortical loop (7, 49). Our proposed interpretation is that the cerebello-thalamo-cortical

597 pathway conveys an estimate of the state of the system that combines an efferent copy of motor  
598 commands with sensory feedback and current estimates that compensates for sensorimotor  
599 delays. When the movement was initiated from a static posture, errors had not yet accumulated  
600 and movement started in the correct direction, but later in the trial, the faulty delay compensation  
601 accumulates errors and the closed-loop system starts producing erroneous control signals  
602 potentially leading to oscillations. This view suggests a very specific cause of tremor in ET patients,  
603 which is linked to errors in real-time state-estimation based on internal feedback of motor  
604 commands. Orienting future research on online feedback control in ET should bring novel insights  
605 to validate or invalidate the hypothesis of impaired delay compensation as candidate root cause of  
606 oscillations in this population.

607 To conclude, our contribution is twofold: on the one hand we replicate the presence of  
608 cerebellar-dependent adaptation deficits in ET population, adding to the line of evidence that this  
609 disorder is linked to cerebellar dysfunction. On the other hand, we proposed a movement  
610 decomposition suggesting a specific functional consequence of the altered cerebellar pathways,  
611 which affects online control more than anticipation.

612

### 613 **Supplemental Data:**

614 Table S1 - Demographic and clinical data of ET patients: DOI: 10.6084/m9.figshare.24072213

615

616

### 617 **5. References**

618

- 619 1. **Louis ED, Ferreira JJ.** How common is the most common adult movement disorder? Update  
620 on the worldwide prevalence of essential tremor. *Mov Disord* 25: 534–541, 2010. doi:  
621 10.1002/mds.22838.
- 622 2. **Bhatia KP, Bain P, Bajaj N, Elble RJ, Hallett M, Louis ED, Raethjen J, Stamelou M, Testa CM,**  
623 **Deuschl G, the Tremor Task Force of the International Parkinson and Movement Disorder**  
624 **Society.** Consensus Statement on the classification of tremors. from the task force on tremor  
625 of the International Parkinson and Movement Disorder Society: IPMDS Task Force on Tremor  
626 Consensus Statement. *Mov Disord* 33: 75–87, 2018. doi: 10.1002/mds.27121.
- 627 3. **Clark LN, Louis ED.** Essential tremor. Elsevier B.V.
- 628 4. **Shanker V.** Essential tremor: Diagnosis and management. *The BMJ* 366, 2019. doi:  
629 10.1136/bmj.l4485.
- 630 5. **Ibrahim MF, Beevis JC, Empson RM.** Essential Tremor – A Cerebellar Driven Disorder?  
631 *Neuroscience* 462: 262–273, 2021. doi: 10.1016/j.neuroscience.2020.11.002.

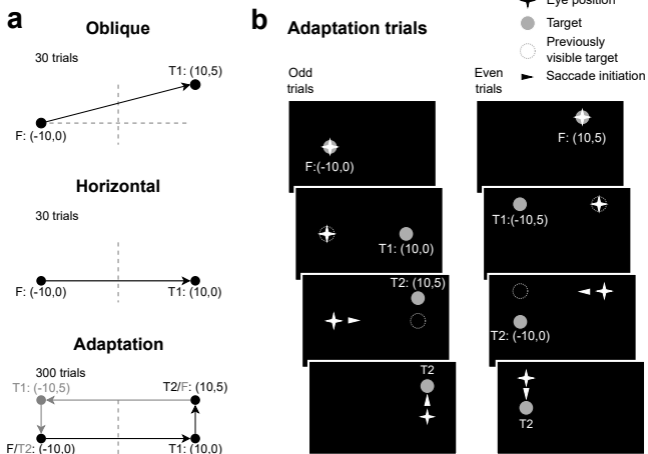
- 632 6. **Mavroudis I, Petrides F, Karantali E, Chatzikonstantinou S, McKenna J, Ciobica A, Iordache**  
633 **AC, Dobrin R, Trus C, Kazis D.** A voxel-wise meta-analysis on the cerebellum in essential  
634 tremor. *Med Lith* 57: 1–10, 2021. doi: 10.3390/medicina57030264.
- 635 7. **Muthuraman M, Raethjen J, Koirala N, Anwar AR, Mideksa KG, Elble R, Groppa S, Deuschl G.**  
636 Cerebello-cortical network fingerprints differ between essential, Parkinson’s and mimicked  
637 tremors. *Brain* 141: 1770–1781, 2018. doi: 10.1093/brain/awy098.
- 638 8. **Pietracupa S, Bologna M, Tommasin S, Berardelli A, Pantano P.** The Contribution of  
639 Neuroimaging to the Understanding of Essential Tremor Pathophysiology: a Systematic  
640 Review. *Cerebellum* , 2021. doi: 10.1007/s12311-021-01335-7.
- 641 9. **Tikoo S, Pietracupa S, Tommasin S, Bologna M, Petsas N, Bharti K, Berardelli A, Pantano P.**  
642 Functional disconnection of the dentate nucleus in essential tremor. *J Neurol* , 2020. doi:  
643 10.1007/s00415-020-09711-9.
- 644 10. **Louis ED, Faust PL.** Essential tremor pathology: neurodegeneration and reorganization of  
645 neuronal connections. *Nat Rev Neurol* 16: 69–83, 2020. doi: 10.1038/s41582-019-0302-1.
- 646 11. **Diedrichsen J, Bastian AJ.** Cerebellar Function. .
- 647 12. **McNamee D, Wolpert DM.** Internal Models in Biological Control. *Annu Rev Control Robot*  
648 *Auton Syst* 2: 339–364, 2019. doi: 10.1146/annurev-control-060117-105206.
- 649 13. **Therrien AS, Bastian AJ.** Cerebellar damage impairs internal predictions for sensory and  
650 motor function. *Curr Opin Neurobiol* 33: 127–133, 2015. doi: 10.1016/j.conb.2015.03.013.
- 651 14. **Kilteni K, Engeler P, Ehrsson HH.** Efference Copy Is Necessary for the Attenuation of Self-  
652 Generated Touch. *iScience* 23: 100843, 2020. doi: 10.1016/j.isci.2020.100843.
- 653 15. **Miall RC, Weir DJ, Wolpert DM, Stein JF.** Is the Cerebellum a Smith Predictor? *J Mot Behav*  
654 25: 203–216, 1993. doi: 10.1080/00222895.1993.9942050.
- 655 16. **Wolpert DM, Miall RC, Kawato M.** Internal models in the cerebellum. *Trends Cogn Sci* 2: 338–  
656 347, 1998. doi: 10.1016/S1364-6613(98)01221-2.
- 657 17. **Miall RC, Christensen LOD, Cain O, Stanley J.** Disruption of state estimation in the human  
658 lateral cerebellum. *PLoS Biol* 5: 2733–2744, 2007. doi: 10.1371/journal.pbio.0050316.
- 659 18. **Baizer JS, Kralj-Hans I, Glickstein M.** Cerebellar Lesions and Prism Adaptation in Macaque  
660 Monkeys. *J Neurophysiol* 81: 1960–1965, 1999. doi: 10.1152/jn.1999.81.4.1960.
- 661 19. **Ojakangas CL, Ebner TJ.** Purkinje cell complex and simple spike changes during a voluntary  
662 arm movement learning task in the monkey. *J Neurophysiol* 68: 2222–2236, 1992. doi:  
663 10.1152/jn.1992.68.6.2222.
- 664 20. **Smith MA, Shadmehr R.** Intact ability to learn internal models of arm dynamics in  
665 Huntington’s disease but not cerebellar degeneration. *J Neurophysiol* 93: 2809–2821, 2005.  
666 doi: 10.1152/jn.00943.2004.

- 667 21. **Tseng YW, Diedrichsen J, Krakauer JW, Shadmehr R, Bastian AJ.** Sensory prediction errors  
668 drive cerebellum-dependent adaptation of reaching. *J Neurophysiol* 98: 54–62, 2007. doi:  
669 10.1152/jn.00266.2007.
- 670 22. **Xu-Wilson M, Chen-Harris H, Zee DS, Shadmehr R.** Cerebellar contributions to adaptive  
671 control of saccades in humans. *J Neurosci* 29: 12930–12939, 2009. doi:  
672 10.1523/JNEUROSCI.3115-09.2009.
- 673 23. **Chen H, Hua SE, Smith MA, Lenz FA, Shadmehr R.** Effects of human cerebellar thalamus  
674 disruption on adaptive control of reaching. *Cereb Cortex* 16: 1462–1473, 2006. doi:  
675 10.1093/cercor/bhj087.
- 676 24. **Bindel L, Mühlberg C, Pfeiffer V, Nitschke M, Müller A, Wegscheider M, Rumpf J-J, Zeuner  
677 KE, Becktepe JS, Welzel J, Güthe M, Classen J, Tzvi E.** Visuomotor Adaptation Deficits in  
678 Patients with Essential Tremor. .
- 679 25. **Hanajima R, Tsutsumi R, Shirota Y, Shimizu T, Tanaka N, Ugawa Y.** Cerebellar dysfunction in  
680 essential tremor. *Mov Disord* 31: 1230–1234, 2016. doi: 10.1002/mds.26629.
- 681 26. **Kronenbuerger M, Gerwig M, Brol B, Block F, Timmann D.** Eyeblink conditioning is impaired  
682 in subjects with essential tremor. *Brain* 130: 1538–1551, 2007. doi: 10.1093/brain/awm081.
- 683 27. **Mathew J, Crevecoeur F.** Adaptive Feedback Control in Human Reaching Adaptation to Force  
684 Fields. *Front Hum Neurosci* 15: 742608, 2021. doi: 10.3389/fnhum.2021.742608.
- 685 28. **Fahn S, Tolosa E, Marin C.** Clinical Rating Scale for Tremor. *Park Dis Mov Disord* 2: 271–280,  
686 1993.
- 687 29. **Córdova Bulens D, Cluff T, Blondeau L, Moore RT, Lefèvre P, Crevecoeur F.** Different Control  
688 Strategies Drive Interlimb Differences in Performance and Adaptation during Reaching  
689 Movements in Novel Dynamics. *eneuro* 10: ENEURO.0275-22.2023, 2023. doi:  
690 10.1523/ENEURO.0275-22.2023.
- 691 30. **Chen-Harris H, Joiner WM, Ethier V, Zee DS, Shadmehr R.** Adaptive control of saccades via  
692 internal feedback. *J Neurosci* 28: 2804–2813, 2008. doi: 10.1523/JNEUROSCI.5300-07.2008.
- 693 31. **Crevecoeur F, Thonnard JL, Lefèvre P.** A very fast time scale of human motor adaptation:  
694 Within movement adjustments of internal representations during reaching. *eNeuro* 7: 1–16,  
695 2020. doi: 10.1523/ENEURO.0394-19.2019.
- 696 32. **Lakens D, Adolphi FG, Albers CJ, Anvari F, Apps MAJ, Argamon SE, Baguley T, Becker RB,  
697 Benning SD, Bradford DE, Buchanan EM, Caldwell AR, Van Calster B, Carlsson R, Chen S-C,  
698 Chung B, Colling LJ, Collins GS, Crook Z, Cross ES, Daniels S, Danielsson H, DeBruine L,  
699 Dunleavy DJ, Earp BD, Feist MI, Ferrell JD, Field JG, Fox NW, Friesen A, Gomes C, Gonzalez-  
700 Marquez M, Grange JA, Grieve AP, Guggenberger R, Grist J, Van Harmelen A-L, Hasselman F,  
701 Hochard KD, Hoffarth MR, Holmes NP, Ingre M, Isager PM, Isotalus HK, Johansson C,  
702 Juszczak K, Kenny DA, Khalil AA, Konat B, Lao J, Larsen EG, Lodder GMA, Lukavský J, Madan  
703 CR, Manheim D, Martin SR, Martin AE, Mayo DG, McCarthy RJ, McConway K, McFarland C,  
704 Nio AQX, Nilsonne G, De Oliveira CL, De Xivry J-JO, Parsons S, Pfuhl G, Quinn KA, Sakon JJ,  
705 Saribay SA, Schneider IK, Selvaraju M, Sjoerds Z, Smith SG, Smits T, Spies JR, Sreekumar V,  
706 Steltenpohl CN, Stenhouse N, Świątkowski W, Vadillo MA, Van Assen MALM, Williams MN,**

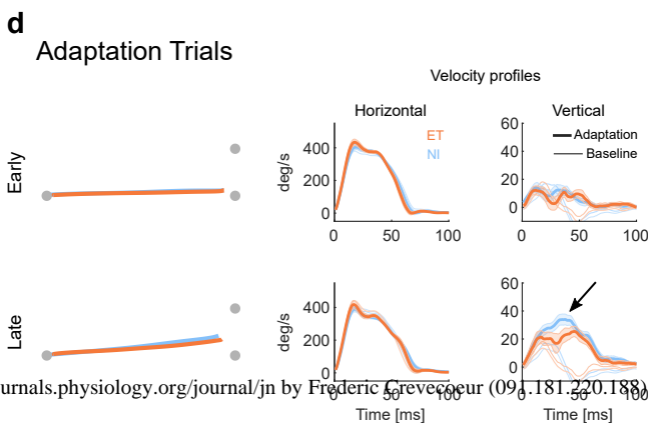
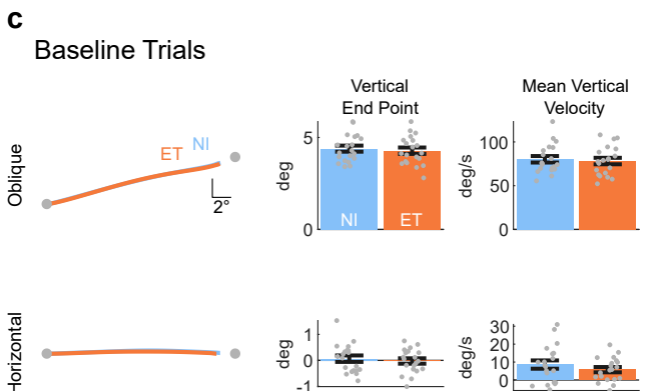
- 707 **Williams SE, Williams DR, Yarkoni T, Ziano I, Zwaan RA.** Justify your alpha. *Nat Hum Behav* 2:  
708 168–171, 2018. doi: 10.1038/s41562-018-0311-x.
- 709 33. **Benjamin DJ, Berger JO, Johannesson M, Nosek BA, Wagenmakers E-J, Berk R, Bollen KA,**  
710 **Brembs B, Brown L, Camerer C, Cesarini D, Chambers CD, Clyde M, Cook TD, De Boeck P,**  
711 **Dienes Z, Dreber A, Easwaran K, Efferson C, Fehr E, Fidler F, Field AP, Forster M, George EI,**  
712 **Gonzalez R, Goodman S, Green E, Green DP, Greenwald AG, Hadfield JD, Hedges LV, Held L,**  
713 **Hua Ho T, Hoijtink H, Hruschka DJ, Imai K, Imbens G, Ioannidis JPA, Jeon M, Jones JH,**  
714 **Kirchler M, Laibson D, List J, Little R, Lupia A, Machery E, Maxwell SE, McCarthy M, Moore**  
715 **DA, Morgan SL, Munafó M, Nakagawa S, Nyhan B, Parker TH, Pericchi L, Perugini M, Rouder**  
716 **J, Rousseau J, Savalei V, Schönbrodt FD, Sellke T, Sinclair B, Tingley D, Van Zandt T, Vazire S,**  
717 **Watts DJ, Winship C, Wolpert RL, Xie Y, Young C, Zinman J, Johnson VE.** Redefine statistical  
718 significance. *Nat Hum Behav* 2: 6–10, 2017. doi: 10.1038/s41562-017-0189-z.
- 719 34. **Helmchen C, Hagenow A, Miesner J, Sprenger A, Rambold H, Wenzelburger R, Heide W,**  
720 **Deuschl G.** Eye movement abnormalities in essential tremor may indicate cerebellar  
721 dysfunction. *Brain* 126: 1319–1332, 2003. doi: 10.1093/brain/awg132.
- 722 35. **Wójcik-Pędziwiatr M, Plinta K, Krzak-Kubica A, Zajdel K, Falkiewicz M, Dylak J, Ober J,**  
723 **Szczudlik A, Rudzińska M.** Eye movement abnormalities in essential tremor. *J Hum Kinet* 52:  
724 53–64, 2016. doi: 10.1515/hukin-2015-0193.
- 725 36. **Van Der Vliet R, Frens MA, De Vreede L, Jonker ZD, Ribbers GM, Selles RW, Van Der Geest**  
726 **JN, Donchin O.** Individual Differences in Motor Noise and Adaptation Rate Are Optimally  
727 Related. *eneuro* 5: ENEURO.0170-18.2018, 2018. doi: 10.1523/ENEURO.0170-18.2018.
- 728 37. **Schween R, McDougale SD, Hegele M, Taylor JA.** Assessing explicit strategies in force field  
729 adaptation. *J Neurophysiol* 123: 1552–1565, 2020. doi: 10.1152/jn.00427.2019.
- 730 38. **Crevecoeur F, Kording KP.** Saccadic suppression as a perceptual consequence of efficient  
731 sensorimotor estimation. *eLife* 6: 1–15, 2017. doi: 10.7554/eLife.25073.
- 732 39. **Lefèvre P, Quaia C, Optican LM.** Distributed model of control of saccades by superior  
733 colliculus and cerebellum. *Neural Netw* 11: 1175–1190, 1998. doi: 10.1016/S0893-  
734 6080(98)00071-9.
- 735 40. **Quaia C, Lefèvre P, Optican LM.** Model of the Control of Saccades by Superior Colliculus and  
736 Cerebellum. *J Neurophysiol* 82: 999–1018, 1999. doi: 10.1152/jn.1999.82.2.999.
- 737 41. **Schreiber C, Missal M, Lefèvre P.** Asynchrony Between Position and Motion Signals in the  
738 Saccadic System. *J Neurophysiol* 95: 960–969, 2006. doi: 10.1152/jn.00315.2005.
- 739 42. **Xu-Wilson M, Tian J, Shadmehr R, Zee DS.** TMS Perturbs Saccade Trajectories and Unmasks  
740 an Internal Feedback Controller for Saccades. *J Neurosci* 31: 11537–11546, 2011. doi:  
741 10.1523/JNEUROSCI.1584-11.2011.
- 742 43. **Bo J, Block HJ, Clark JE, Bastian AJ.** A Cerebellar Deficit in Sensorimotor Prediction Explains  
743 Movement Timing Variability. *J Neurophysiol* 100: 2825–2832, 2008. doi:  
744 10.1152/jn.90221.2008.

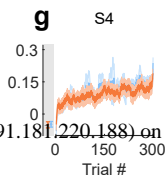
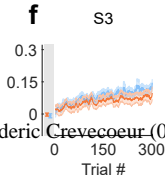
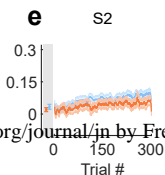
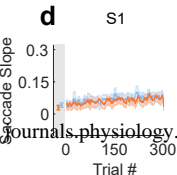
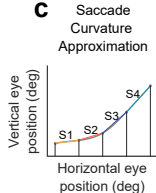
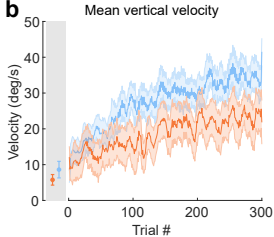
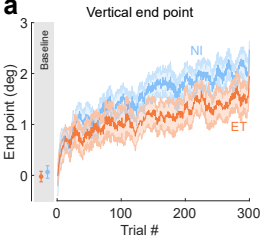
- 745 44. **Diedrichsen J, Criscimagna-Hemminger SE, Shadmehr R.** Dissociating Timing and  
746 Coordination as Functions of the Cerebellum. *J Neurosci* 27: 6291–6301, 2007. doi:  
747 10.1523/JNEUROSCI.0061-07.2007.
- 748 45. **Kilteni K, Houborg C, Ehrsson HH.** Rapid learning and unlearning of predicted sensory delays  
749 in self-generated touch. *eLife* 8: e42888, 2019. doi: 10.7554/eLife.42888.
- 750 46. **Martin TA, Keating JG, Goodkin HP, Bastian AJ, Thach WT.** Throwing while looking through  
751 prisms: I. Focal olivocerebellar lesions impair adaptation. *Brain* 119: 1183–1198, 1996. doi:  
752 10.1093/brain/119.4.1183.
- 753 47. **Crevecoeur F, Gervers M.** Filtering compensation for delays and prediction errors during  
754 sensorimotor control. 2954: 2925–2954, 2019. doi: 10.1162/NECO.
- 755 48. **Stein RB, Ögüztörel MN.** Tremor and other oscillations in neuromuscular systems. *Biol*  
756 *Cybern* 22: 147–157, 1976. doi: 10.1007/BF00365525.
- 757 49. **Helmich RC, Toni I, Deuschl G, Bloem BR.** The pathophysiology of essential tremor and  
758 parkinson’s tremor. *Curr Neurol Neurosci Rep* 13, 2013. doi: 10.1007/s11910-013-0378-8.
- 759

# Protocol design

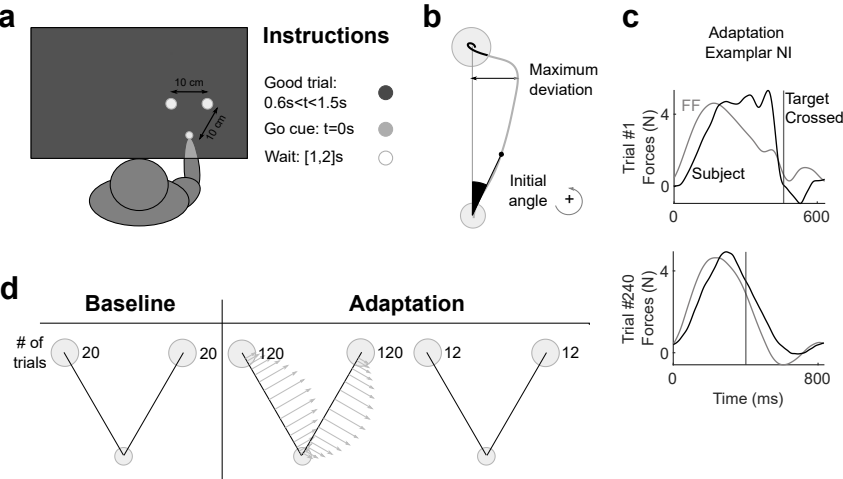


# Participants' behavior

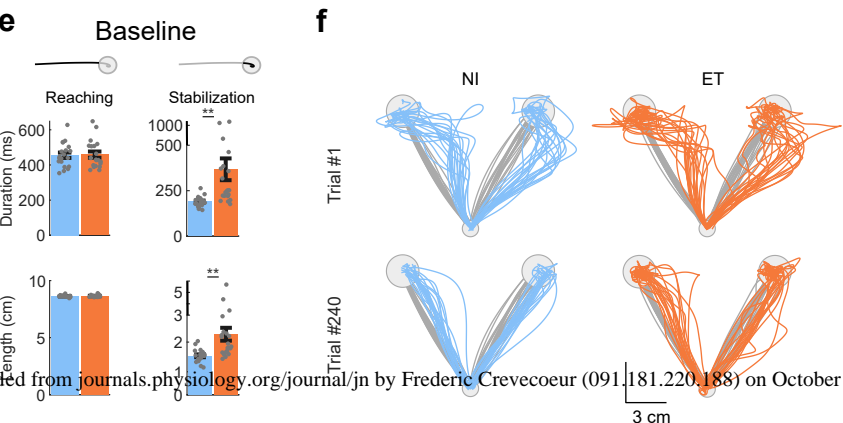


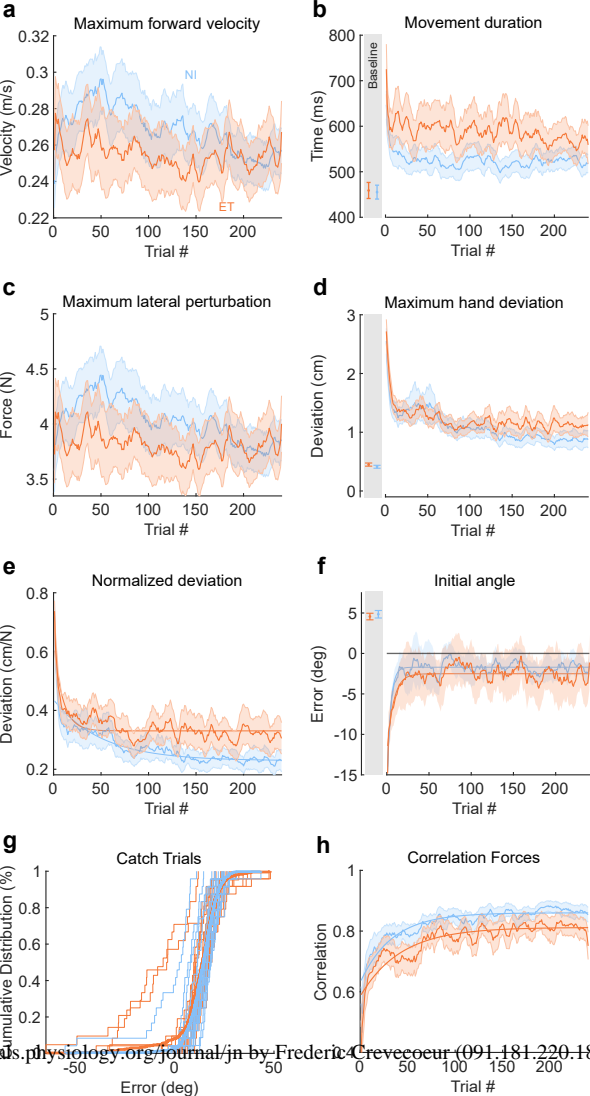


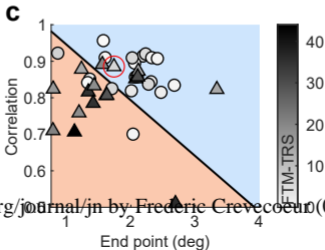
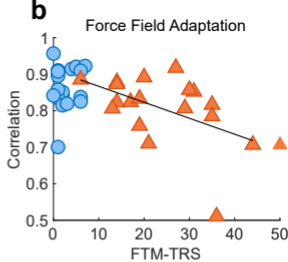
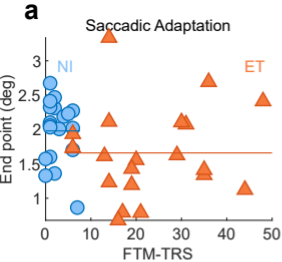
# Protocol design



# Participants' behavior

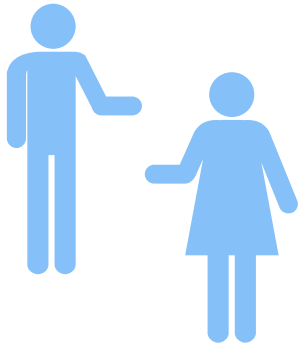




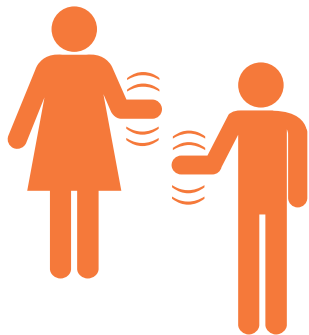


## Participants

20 Neurologically Intact Volunteers



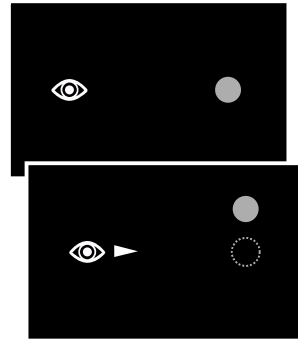
20 Essential Tremor Patients



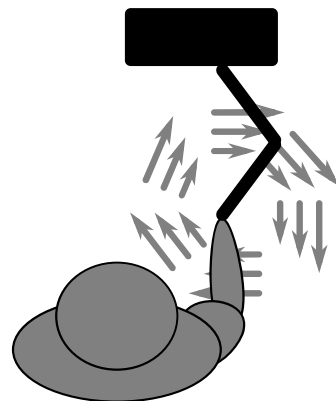
## The tasks



Peri-Saccadic Target Jump

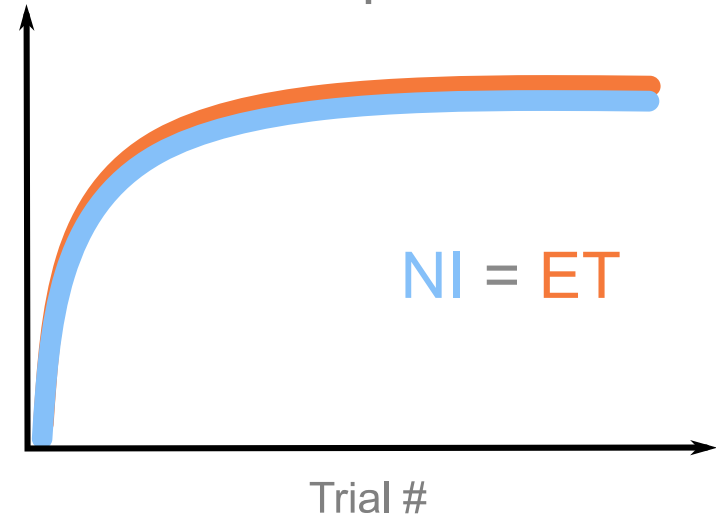


Force field perturbation



## Adaptation

### Anticipation



### Control

